

<https://doi.org/10.1038/s42003-024-06725-1>

Peptide-mimetic treatment of *Pseudomonas aeruginosa* in a mouse model of respiratory infection

Check for updates

Madeleine G. Moule^{1,2,6}, Aaron B. Benjamin^{1,6}, Melanie L. Buger², Claudine Herlan³, Maxim Lebedev¹, Jennifer S. Lin⁴, Kent J. Koster¹, Neha Wavare¹, Leslie G. Adams⁵, Stefan Bräse³, Ricardo Munoz-Medina¹, Carolyn L. Cannon¹, Annelise E. Barron⁴✉ & Jeffrey D. Cirillo¹✉

The rise of drug resistance has become a global crisis, with >1 million deaths due to resistant bacterial infections each year. *Pseudomonas aeruginosa*, in particular, remains a serious problem with limited solutions due to complex resistance mechanisms that now lead to more than 32,000 multidrug-resistant (MDR) infections and over 2000 deaths in the U.S. annually. While the emergence of resistant bacteria has become ominously common, identification of useful new drug classes has been limited over the past over 40 years. We found that a potential novel therapeutic, the peptide-mimetic TM5, is effective at killing *P. aeruginosa* and displays sufficiently low toxicity in mammalian cells to allow for use in treatment of infections. Interestingly, TM5 kills *P. aeruginosa* more rapidly than traditional antibiotics, within 30–60 min in vitro, and is effective against a range of clinical isolates, including extensively drug resistant strains. In vivo, TM5 significantly reduced bacterial load in the lungs within 24 h compared to untreated mice and demonstrated few adverse effects. Taken together, these observations suggest that TM5 shows promise as an alternative therapy for MDR *P. aeruginosa* respiratory infections.

The rising prevalence of antimicrobial resistance (AMR) has resulted in a resurgence of bacterial diseases that would otherwise have been successfully treated with antibiotics. In 2019, the WHO reported that at least 700,000 people die each year due to drug-resistant diseases and predicted that this number could rise to 10 million deaths per year by 2050¹. A surveillance report by the European Center for Disease Control (ECDC) using data from 2021 reported that 6 of 44 countries in Europe had antimicrobial resistance rates over 50% while only 2 of 44 European countries had rates less than 5%². The American Center for Disease Control (CDC) outlined the biggest AMR threats to the United States in a 2019 report, one of which is the facultative aerobic *Pseudomonas aeruginosa*³.

P. aeruginosa is a ubiquitous, opportunistic pathogen which utilizes over 100 different organic molecules for energy acquisition via carbon or as a prototroph⁴. One significant problem with treatment of *P. aeruginosa* infections is the ability of the bacteria to develop antibiotic resistance quickly via both horizontal gene transfer and mutations which lead to up-regulation

of β -lactamases and efflux pumps^{4,5}. The most severe *Pseudomonas* infections include respiratory infections in patients with cystic fibrosis and systemic bloodstream infections that have disseminated from burn wounds or pneumonia^{5,6}. In the United States alone, it was estimated that over 30,000 multidrug-resistant cases were seen in 2019, with estimated healthcare associated costs of \$750 million in 2017³. Due to this increase in resistance, there is an urgent need to develop new antimicrobials against *P. aeruginosa* which can bypass traditional resistance mechanisms.

The current frontline treatments for infections with *P. aeruginosa* encompass a variety of different antibiotic classes, including aminoglycosides, carbapenems, cephalosporins, fluoroquinolones, penicillins with β -lactamases, monobactams, and fosfomycin with polymyxins as a last resort^{5,7,8}. Despite this diversity of options, misuse of antibiotics and non-compliance has increased the amount of drug resistance observed in clinical infections and resulted in the emergence of multidrug resistant (MDR) strains. Additionally, since the golden era of antibiotic discovery ended in

¹Department of Microbial Pathogenesis and Immunology, Texas A&M School of Medicine, Bryan, TX, USA. ²Institute of Immunology & Infection Research, School of Biological Sciences, University of Edinburgh, Edinburgh, UK. ³Institute of Biological and Chemical Systems - Functional Molecular Systems (IBCS-FMS), Karlsruhe Institute of Technology (KIT), Karlsruhe, Germany. ⁴Department of Bioengineering, Stanford University Schools of Medicine and of Engineering, Stanford, CA, USA. ⁵Department of Veterinary Pathobiology, Texas A&M School of Veterinary Medicine & Biomedical Sciences, College Station, TX, USA. ⁶These authors contributed equally: Madeleine G. Moule, Aaron B. Benjamin. ✉e-mail: aebarron@stanford.edu; jdcirillo@tamu.edu

the 1960s, traditional approaches to drug discovery have yielded fewer new classes of antimicrobials each subsequent year^{9–11}. While new antibiotic development has been stuck at a snail's pace, the bacterial world has continued to evolve and develop resistances at an alarming rate, resulting in a wide range of mechanisms through which bacteria can overcome antimicrobial burden. Examples include, but are not limited to, efflux pumps, modification of antibiotics, changes in the membrane to prevent drug penetration, and target modification^{9,12}. To bypass these methods of resistance, alternative strategies need to be explored for drug development, such as utilizing natural host-based immunity via biomimetics.

One family of promising antibiotic alternatives are antimicrobial peptides (AMPs). AMPs exhibit an extensive spectrum of applications and a lower risk of resistance development compared to traditional antibiotics, making them promising candidates as next-generation antibiotics¹³. AMPs, also called host defense peptides, are produced by nearly all organisms from prokaryotes to humans as products of the innate immune system. Most AMPs are short cationic amphiphilic peptides and display activity against a broad range of pathogens including bacteria, viruses, and fungi¹⁴. They have also demonstrated anticancer properties¹⁵, have been seen as chemoattractants¹⁶, and can modulate the inflammatory response^{17–19}. In humans, endogenous AMPs are grouped into three families based on their structural homology motifs: defensins, cathelicidins and histatins^{20–24}. In humans, there is only one known cathelicidin, the host defense peptide LL-37^{25,26}. LL-37 is involved in a variety of functions, including both direct microbicidal activities and immunomodulatory functions^{18,19,27–33}. Unfortunately, LL-37 is not able to eliminate all bacterial infections by itself, and resistance against some natural antimicrobial peptides has begun to increase³⁴. Additionally, their low bioavailability and susceptibility to degradation by proteases in vivo reduces their therapeutic potential. Despite this, their efficacy against both gram-positive and gram-negative bacteria, including antibiotic resistant strains, makes AMPs potential scaffolds for the design of mimics capable of treating infections³⁵.

Since AMPs are easily manipulated and their structures are so tightly connected to their efficacy, creating peptidomimetics provides an untapped reservoir of antimicrobial therapeutic solutions. We have previously developed a class of AMP derivatives known as peptoids, or *N*-substituted glycine oligomer peptidomimetics, based off LL-37^{36–39}. Peptoids differ from peptides in that the side chains are linked to the amide in the backbone instead of the α -carbon. This change in structure removes hydrogen bonding from the backbone and makes peptoids resistant to proteolysis. Here, we focus on the therapeutic potential of the peptoid TM5 against *P. aeruginosa*. We have shown that TM5 is a promising candidate for treatment of *P. aeruginosa* infections due to its potent antimicrobial activity against this organism, improved stability compared to the parental AMP, and low toxicity to the host.

Results

Peptoid TM5 is an effective antimicrobial against *P. aeruginosa* Xen41

AMPs have previously demonstrated potent antimicrobial activity in vitro against a wide range of gram-negative and gram-positive bacteria^{40–42}. To evaluate the efficacy of our peptoids against *P. aeruginosa*, we first determined the minimum inhibitory concentration (MIC) and minimum bactericidal concentration (MBC) of TM5 against the bioluminescent strain Xen41, a luminescent derivative of *P. aeruginosa* PAO1 that contains an integrated LuxABCDE operon cloned from *Photobacterium luminescens*^{43,44}. Overnight cultures of Xen41 were treated with 0–64 $\mu\text{g}/\text{mL}$ of either TM1, TM5, TM6, ceftazidime, ciprofloxacin, kanamycin, or meropenem. The MIC₉₀ for TM1 and TM5 were determined to be 4–8 and 4 $\mu\text{g}/\text{mL}$, respectively, while the MIC₉₀ for TM6 was 16 $\mu\text{g}/\text{mL}$ (Fig. 1, Table 1).

To determine the MBC, an indicator of bacterial killing rather than growth inhibition, bacterial colony forming units (CFU) were enumerated. The MBC of TM1 and TM6 were 8 and 32 $\mu\text{g}/\text{mL}$ respectively, (Fig. 1, Table 1). For TM5, the MBC was determined to be between 2–16 $\mu\text{g}/\text{mL}$, as the CFUs/mL hovered at the MBC threshold of 95% killing at all

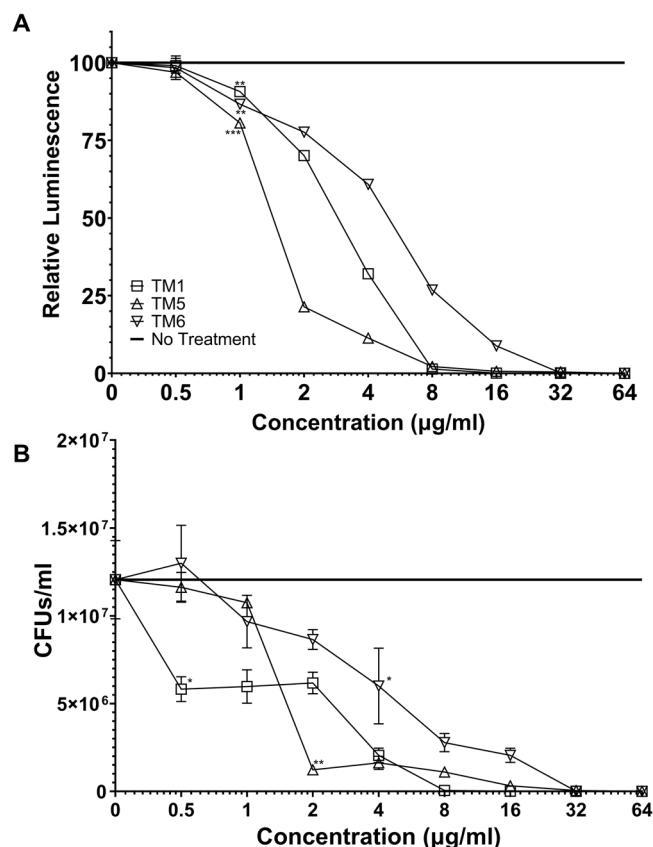


Fig. 1 | Bactericidal activity of Peptoids TM1, TM5, and TM6. Relative luminescence (A) and CFUs/mL (B) for *P. aeruginosa* Xen41 treated with 2-fold dilutions of TM1, TM5, and TM6. A TM1, TM5, and TM6 were all significantly different from the no treatment control with respect to their relative luminescence at concentrations of 1 $\mu\text{g}/\text{mL}$ and higher. B TM1 was significantly different from the no treatment control for CFUs/mL at concentrations of 0.5 $\mu\text{g}/\text{mL}$ and above, while TM5 and TM6 were significantly different at 2 and 4 $\mu\text{g}/\text{mL}$ respectively. Data points are represented as means (n =replicates). Error is shown in \pm standard deviation (SD). Statistics were performed using 2-way ANOVA, comparing antimicrobial to no treatment control. *P* values are: <0.001 = ***, between 0.001 and 0.01 = **, and between 0.01 and 0.05 = *.

Table 1 | MICs and MBC of peptoids against *P. aeruginosa* Xen41

Peptoid	Sequence	MBC	MIC ₅₀	MIC ₉₀
TM1	H-(NLys-Nspe-Nspe) ₄ -NH ₂	8 $\mu\text{g}/\text{mL}$	2–4 $\mu\text{g}/\text{mL}$	4–8 $\mu\text{g}/\text{mL}$
TM5	H-Ntridec-NLys-Nspe-Nspe-NLys-NH ₂	2–16 $\mu\text{g}/\text{mL}$	1–2 $\mu\text{g}/\text{mL}$	4 $\mu\text{g}/\text{mL}$
TM6	H-(NLys-Nspe-Nspe) ₃ -NLys-Nspe-NH ₂	32 $\mu\text{g}/\text{mL}$	4–8 $\mu\text{g}/\text{mL}$	16 $\mu\text{g}/\text{mL}$

concentrations within that range (Fig. 1). TM1 showed a significant decrease in CFUs at concentrations higher than 0.5 $\mu\text{g}/\text{mL}$, TM5 at concentrations higher than 2 $\mu\text{g}/\text{mL}$, and TM6 at concentrations higher than 4 $\mu\text{g}/\text{mL}$. As a control, the antibiotics ceftazidime, ciprofloxacin, kanamycin, and meropenem were all tested in the same manner. Ciprofloxacin showed the lowest MIC₉₀, and MBC, and 2–4 $\mu\text{g}/\text{mL}$ Kanamycin showed consistent MIC₉₀ and MBC of >64 $\mu\text{g}/\text{mL}$, while meropenem had an MIC₉₀ of 1 $\mu\text{g}/\text{mL}$ and an MBC of 2 $\mu\text{g}/\text{mL}$ (Fig. 2, Table 2)

TM5 demonstrates consistent efficacy against drug resistant clinical isolates of *P. aeruginosa*

P. aeruginosa PAO1, the parental strain from which Xen41 was derived, was originally a clinical isolate derived from a wound infection in an

Australian patient in 1954. However, due to the genetic plasticity of *P. aeruginosa*, it is well documented that continuous propagation has resulted in laboratory strains demonstrating significant differences in virulence and antibiotic resistance profiles compared to direct clinical isolates^{45,46}. To determine if our peptoids retain the ability to effectively kill clinical strains from diverse sources with different AMR profiles, we

tested our most promising candidate, TM5, against strains from the Kolter collection including a second laboratory strain from this collection that demonstrates increased virulence (PA14), and clinical isolates originating from trachea (PAZK69), wound (PAZK2019), and cystic fibrosis lung infections (PAZK2870)^{47,48}. Although these strains have a variety of antibiotic susceptibility profiles, every strain demonstrated consistent susceptibility to peptoid TM5 with a MIC of 8 µg/mL (Table 3). To evaluate the efficacy of TM5 against antibiotic resistant strains from a variety of lineages, additional clinical isolates with established resistance profiles were obtained and tested against all three peptoids (Fig. S3)⁴⁹. These strains had previously been determined to be resistant to a variety of frontline drugs and represent a range of virulence phenotypes⁴⁹. All strains tested showed similar MIC and MBC values for TM5 when compared to Xen41 and in some strains TM5 is even more effective at lower concentrations than for Xen41.

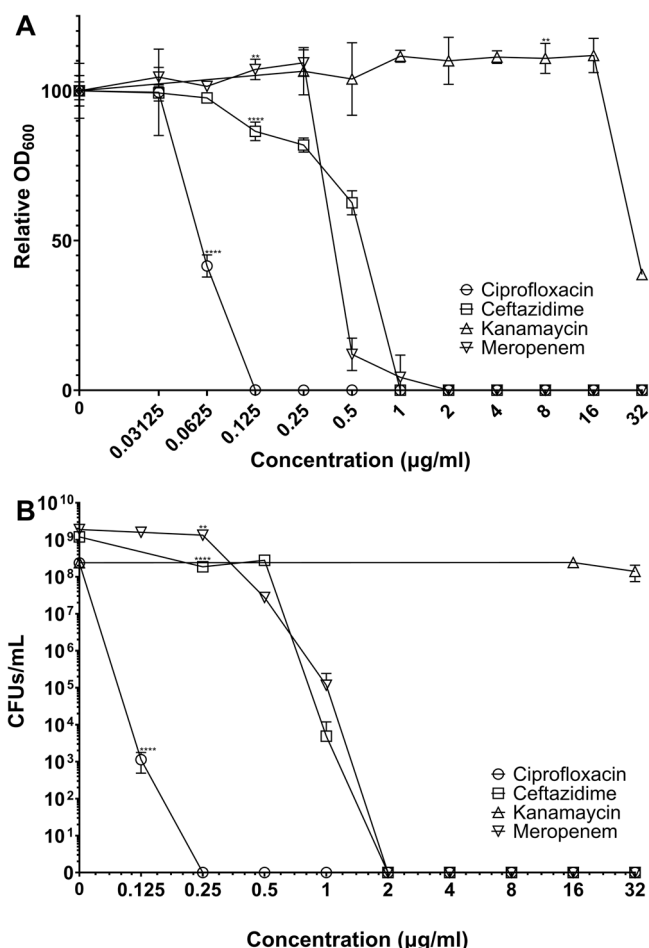


Fig. 2 | Bactericidal of standard antibiotics. Relative OD₆₀₀ (A) and CFUs/ml (B) for *P. aeruginosa* Xen41 with 2-fold dilutions of ciprofloxacin, ceftazidime, kanamycin, and meropenem. A Ciprofloxacin was significantly different above concentrations of 0.0625 µg/ml and above. Ceftazidime and meropenem were significantly different at concentrations above 0.125 µg/ml, while kanamycin was significantly different at concentrations of 8 µg/ml and above. B Ciprofloxacin showed a significant decrease compared to the no treatment control for CFUs/ml at all concentrations, while ceftazidime and meropenem were significantly different at 0.25 µg/ml and above. Kanamycin didn't show any significant difference at any concentrations. Data points are represented as means using four replicates. Error is shown in ± standard deviation (SD). Statistics were performed using 2-way ANOVA, comparing antimicrobial to no treatment control. P values are: <0.0001 = ****, between 0.0001 and 0.001 = ***, between 0.001 and 0.01 = **, and between 0.01 and 0.05 = *.

Peptoid TM5 kills *P. aeruginosa* Xen41 faster than traditional antibiotics

P. aeruginosa Xen5 was previously tested against various peptoids to determine the bacterial killing kinetics⁵⁰. As Xen41 belongs to a different genetic lineage, we performed time-kill experiments to verify that the kinetics are similar across *P. aeruginosa* strains⁵¹. Bacteria treated with TM5 showed a reduction in luminescence after 5 minutes, for all concentrations greater than 4 µg/mL. After 45 min, there was near complete killing for concentrations of 16 µg/mL and above, while concentrations of 8 µg/mL appeared to inhibit growth (Fig. 3A). In comparison, treatment with the control antibiotic ciprofloxacin showed no reduction of luminescence within the entire 120 min timeframe (Fig. 3B). Interestingly, TM1 treatment decreased luminescence immediately at concentrations of 8 µg/mL and higher, with a consistent decrease at 4 µg/mL after 30 min. TM6 treatment decreases luminescence at concentrations of 16 µg/mL and higher starting at 5 min and shows some level of stagnation at 8 µg/mL (Fig. S1b). The gold standard antibiotic ceftazidime did not show a reduction of luminescence for any concentration of drug tested during the 120 min time frame (Fig. S2a). Kanamycin showed a slight reduction from 60 min onward at 64 µg/mL while meropenem showed a limited decrease in luminescence after 60 min for most concentrations after 60 min (Fig. S2b, c). As such, all three peptoids showed a reduction in luminescence much faster than traditionally utilized antibiotics.

Resistance to TM5 does not develop during laboratory evolution experiments

To determine whether antimicrobial resistance to peptoids TM5 could readily emerge under sufficient evolutionary pressure, laboratory evolution experiments were performed. *P. aeruginosa* PAO1 was serially passaged in increasing concentrations of peptoids TM5 or the antibiotic ciprofloxacin as a control until no growth was observed in cultures containing TM5 above 4.5 µg/mL and the evolved strains were evaluated by MIC assay. As expected, resistance to ciprofloxacin emerged quickly under this selective pressure, with the MIC increasing from 0.125 µg/mL to 8 µg/mL over the course of the experiment (Fig. 4A). However, no increase in MIC was observed in strains passaged in TM5 under the same conditions, suggesting a lack of resistance emergence (Fig. 4B). To further determine whether TM5 is effective against fully drug resistant strains, MIC assays were performed on the newly evolved ciprofloxacin-resistant strains. However, no increase

Table 2 | MICs and MBC of traditional antibiotics against *P. aeruginosa* Xen41

Antibiotic	Sequence	MBC	MIC ₅₀	MIC ₉₀
Ciprofloxacin	C ₁₇ H ₁₈ FN ₃ O ₃	0.25 µg/ml	0.03125–0.0625 µg/ml	0.0625–0.125 µg/ml
Ceftazidime	C ₂₂ H ₂₂ N ₆ O ₇ S ₂	2 µg/ml	0.5–1 µg/ml	0.5–1 µg/ml
Kanamycin	C ₁₈ H ₃₆ N ₄ O ₁₁	>32 µg/ml	16–32 µg/ml	>32 µg/ml
Meropenem	C ₁₇ H ₂₅ N ₃ O ₅ S	2 µg/ml	0.25–0.5 µg/ml	0.5 µg/ml

Table 3 | MICs of TM5 and traditional antibiotics against clinical strains of *P. aeruginosa*

Peptoid/Antibiotic	Sequence	MIC				
		PA14	PAZK2870	PAZK2019	PAZK69	PAZK3095
TM5	H-Ntridec-NLys-Nspe-Nspe-NLys-NH ₂	8 µg/ml	8 µg/ml	8 µg/ml	8 µg/ml	-
Ciprofloxacin	C ₁₇ H ₁₈ FN ₃ O ₃	0.125 µg/ml	0.125 µg/ml	0.125 µg/ml	0.06 µg/ml	0.25 µg/ml
Ceftazidime	C ₂₂ H ₂₂ N ₆ O ₇ S ₂	2 µg/ml	2 µg/ml	2 µg/ml	1 µg/ml	1 µg/ml
Kanamycin	C ₁₈ H ₃₆ N ₄ O ₁₁	32 µg/ml	64 µg/ml	64 µg/ml	32 µg/ml	64 µg/ml
Meropenem	C ₁₇ H ₂₅ N ₃ O ₅ S	0.5 µg/ml	1 µg/ml	1 µg/ml	2 µg/ml	0.5 µg/ml

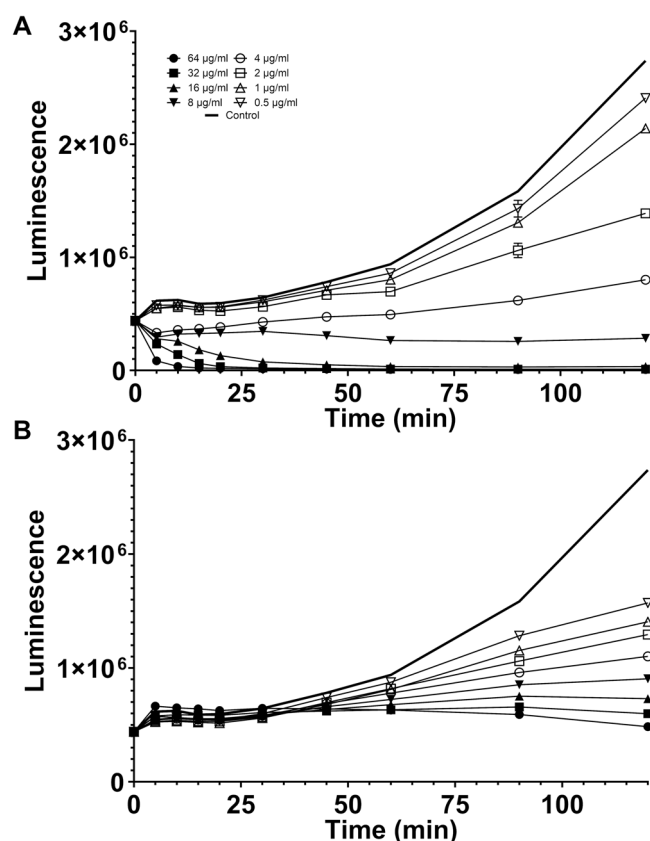


Fig. 3 | Comparative time-kill experiments of Peptoid TM5 and ciprofloxacin. Time course experiments for 2-fold dilutions of TM5 (A) and ciprofloxacin (B) mixed with *P. aeruginosa* Xen41 were measured for luminescence at the following time points: 0, 5, 10, 15, 20, 30, 45, 60, 90, and 120 min. In addition to 2-fold dilutions, a control with PBS was also measured (*n* = 4 replicates).

in MIC was observed and TM5 was equally effective against these evolved strains (Fig. 4C).

TM5 treatment is well-tolerated by mammalian cells

We next evaluated the effects of peptoid treatment on mammalian cells in vitro. TM5 was well-tolerated by A549 cells compared to TM1 and TM6, showing no cytotoxicity after 3 h of treatment with doses at or below 64 µM using an MTS cell viability assay (Fig. S4). We further tested the cells using an Alamar Blue assay to examine whether the cells were actively producing energy after 24 h of peptoid treatment and only saw mild effects on cell growth at concentrations below 32 µg/mL (Fig. 5A). This provided a large enough therapeutic window to justify further investigation of the effects of peptoids on mammalian cells. When comparing the median toxic dose (TD50), TM5 had the highest value at approximately 52 µg/mL, TM6 had the next highest value at approximately 24.5 µg/mL, and TM1 had the lowest value at approximately 17 µg/mL.

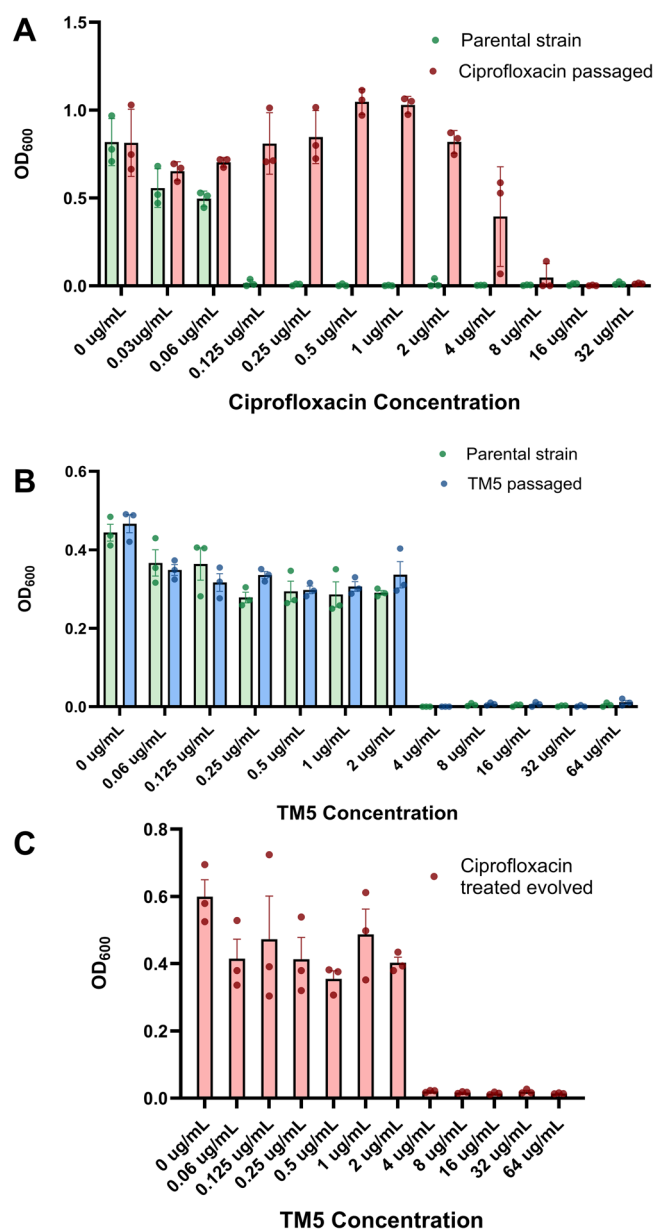


Fig. 4 | Resistance to Peptoid TM5 could not be derived through laboratory evolution. *P. aeruginosa* PAO1 was serially passaged in increased concentrations of either A ciprofloxacin or B peptoids TM5. After 3 weeks of successive passaging in concentrations doubling weekly from 0.5XMIC-2XMIC, resistance of ciprofloxacin had readily emerged with the MIC increasing from 0.125 µg/mL to 8 µg/mL. In contrast, no increase in MIC was observed for peptoid TM5. To evaluate whether TM5 was effective against drug resistant strains, the newly evolved ciprofloxacin-resistant isolates were tested against peptoids TM5 (C), which was found to be equally effective with a MIC of 4 µg/mL.

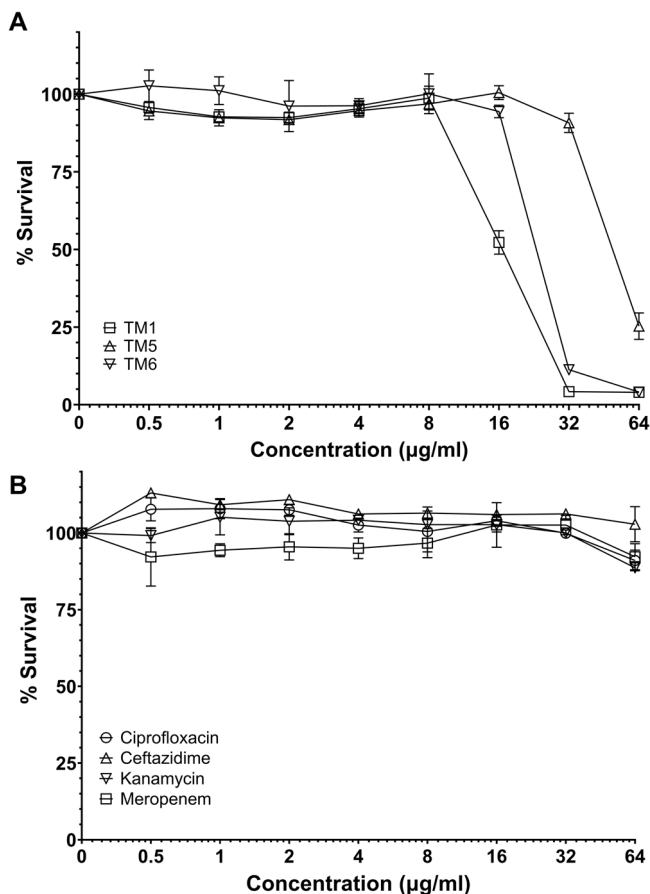


Fig. 5 | Cytotoxicity of Peptoids TM1, TM5, and TM6 on mammalian cells. An Alamar Blue assay was used to determine the effects of 24 h treatment with 2-fold dilutions of each peptoid (A) or standard frontline antibiotic (B) on the viability of A549 human lung epithelial cells. All concentrations and conditions were tested in triplicate, with error is shown as standard deviation.

Development of tissue culture models of the mammalian lung for peptoid characterization

Although our initial data on the cytotoxicity of TM5 on mammalian cells was promising, standard tissue culture is not particularly well-representative of how cells behave within a living organism. To better understand how the peptoid TM5 interacts with cells within the lung, we developed and tested three-dimensional models of the alveolar epithelia. We first assayed a spheroid model of A549 human lung epithelial cells, simple organoids consisting of a single cell type grown as a scaffold-free three-dimensional model. Spheroids have previously been used extensively to study the delivery and toxicity of many novel cancer drugs as the pharmacokinetics and pharmacodynamics observed in these models more closely represent what is seen in vivo⁵²⁻⁵⁴. More recently, they have also been used as models of viral pathogenesis as these multicellular clusters provide an ideal platform to observe viral growth and replication in a more complex microenvironment⁵⁵. Spheroids were assayed by microscopy to confirm their integrity (Fig. 6A), and MTS assays were performed. Under these conditions TM5 treatment resulted in decreased cytotoxicity, with only minimal cell death observed at a concentration of 240 µg/mL (Fig. 6C).

Next, we sought to examine how epithelial cells would be affected by peptoid treatment in conditions where they are exposed to air to mimic the oxygen exchange environment in mammalian lungs using air-liquid interface (ALI) culture methods. ALI culture promotes differentiation of the epithelium, causing the cells to become ciliated, secrete increased extracellular matrix, and form more established tight junctions to create a tight barrier capable of excluding foreign materials. Z-stack images of these cultures show distinct cell junctions and thick cuboidal phenotypes (Fig. 6B). When the same cytotoxicity assay was performed on ALI cultures, no cytotoxicity was observed at any concentration tested, suggesting that the differentiated cells were protected from adverse effects when grown in conditions that best mimic the lung environment (Fig. 6C). To further confirm this, we tested the barrier function of the ALI cultures using a dextran diffusion assay. After three hours of treatment with TM5, no change in barrier function is observed at any concentration of TM5 for larger molecules and only a slight difference is observed at 200 µM for small molecules, confirming that the A549 cells remained alive and able to perform their primary protective function (Fig. 6D).

Fig. 6 | Cytotoxicity of Peptoid TM5 in three-dimensional models of the human lung.

A549 cells were grown in three-dimensional models of the human lung in the form of A spheroid cultures or B air-liquid interface (ALI) cultures. C Culturing A549 cells under conditions which mimic an in vivo lung environment result in decreased cytotoxicity following peptoid treatment as measured by MTS assay. D Integrity of the barrier function of ALI monolayers following peptoid treatment with no significant difference in dextran diffusion observed at 200 µM concentrations or below. Dextran Alexa FluorTM 488 was used for the 3000 Da exclusion and Dextran Alexa FluorTM 647 was used for the 10,000 Da exclusion. Statistics were performed using 2-way ANOVA, using Šidák's multiple comparisons test to compare sample means, with standard error mean (SEM). P values represented as: <0.0001 = ****, between 0.0001 and 0.001 = ***, between 0.001 and 0.01 = **, and between 0.01 and 0.05 = *.

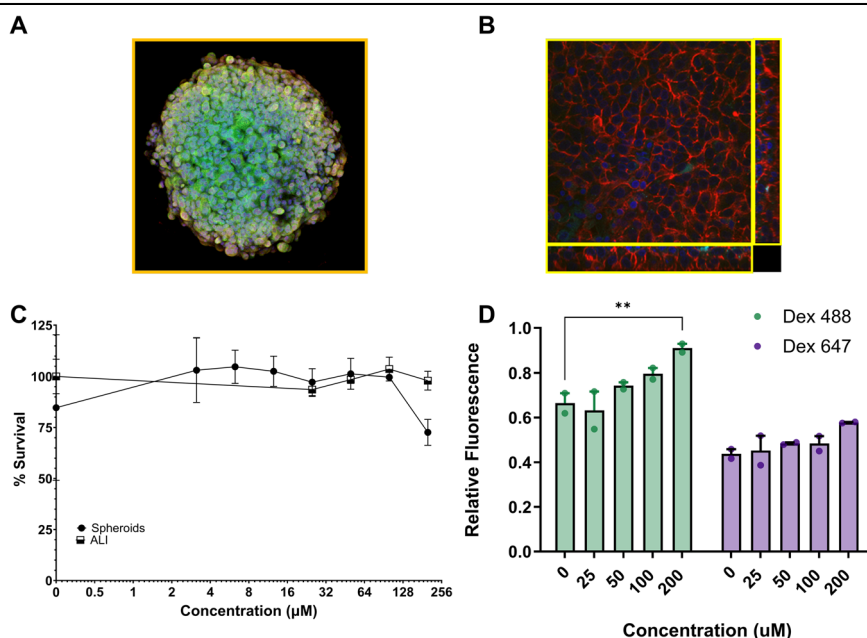
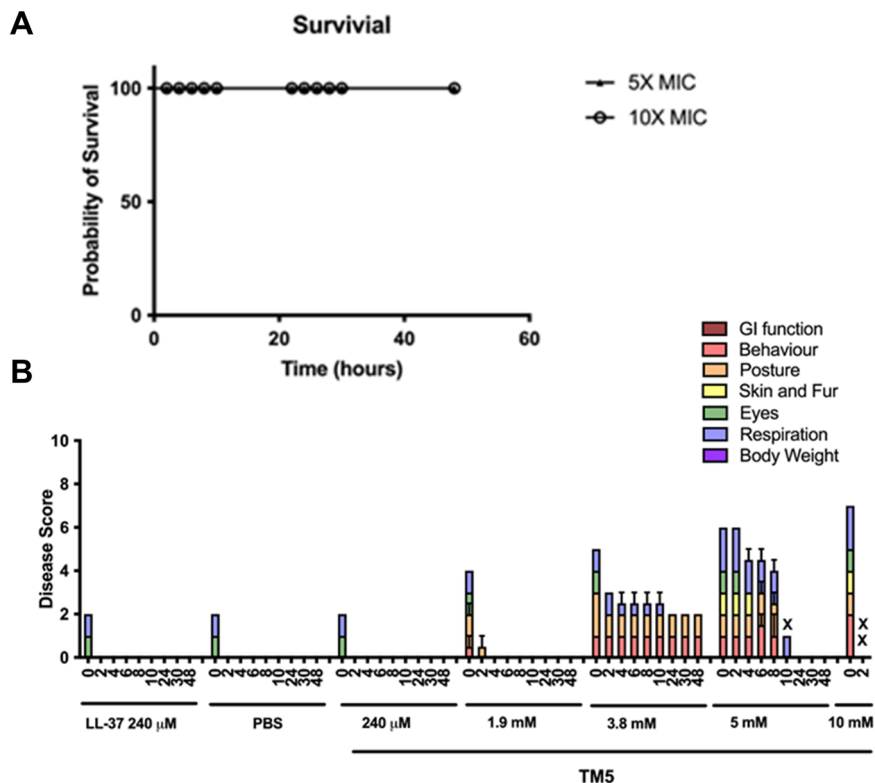


Fig. 7 | In vivo Toxicity of Peptoid TM5 following intratracheal delivery. **A** BALB/c mice were treated with 50 μ L of either 40 μ g/mL (\blacktriangle) or 80 μ g/mL (\circ) doses of TM5 and monitored for survival at 0, 2, 4, 6, 8, 10, 24, 30, and 48 h post-treatment ($n = 2$ mice per concentration). **B** BALB/c mice were treated with increasing doses of TM5 to determine a toxicity threshold and monitored for disease symptoms at 0, 2, 4, 6, 8, 10, 24, 30, and 48 h post-treatment as indicated below the X-axis. Error bars represent SEM across $n = 4$ mice, and timepoints marked with an X indicated animals humanely euthanized at that timepoint.



Intratracheal treatment with TM5 is safe and results in minimal adverse effects in vivo

Having established that TM5 causes extremely low cytotoxicity to mammalian cells cultured in three-dimensional models, we predicted it would demonstrate similarly low toxicity in vivo. Using a BALB/c mouse model, we initially inoculated a small number of animals with 50 μ L of TM5 via the intratracheal route using doses that represented 5X and 10X the in vitro MIC for *P. aeruginosa* Xen41 (40 μ g/mL and 80 μ g/mL). These doses would be predicted to kill or inhibit bacterial growth without causing significant cytotoxicity to host cells. Indeed, we observed 100% survival of all animals following two rounds of treatment 24 h apart, with no observable adverse effects on the animals' health or well-being (Fig. 7A).

To determine the maximum safe dosage of TM5, we next treated animals with increasing intratracheal doses of the peptoid alongside a PBS control and the parental peptide LL-37. Animals were monitored every hour following treatment and scored using a modified Karnofsky score for behavior, posture, weight, temperature, breathing, and physical appearance (Table S1). At approximately 40 μ g/mL, our proposed therapeutic dosage, no effects above those seen in the controls were observed, and all animals appeared healthy and active within 30 minutes of treatment (Fig. 7B). Even at concentrations 10-fold higher, minimal adverse effects were observed, with a gradual increase in adverse effects observed with increasing concentrations of TM5 up to an LD₅₀ of approximately 20 mg/mL. We therefore concluded that TM5 is safe in vivo use at over 2500X MIC concentrations.

Peptoid TM5 significantly reduces bacterial load in the lungs of infected mice compared to other peptoids

Since TM5 was well-tolerated when administered to the lungs in mice, we next tested the efficacy of TM5 in vivo against *P. aeruginosa* lung infections. Groups of 8 BALB/c mice were treated with either TM1, TM5, TM6, or ciprofloxacin alongside ten untreated controls and 4 uninfected control mice. Mice were monitored carefully following treatment, recording modified Karnofsky scores for each mouse over the course of the 3-day experiment (Fig. 8). Untreated mice showed the highest disease scores on

average at both 24 and 48 h post-infection. Both TM1 and TM5 mice showed mild disease scores which decreased after 24 h (Fig. 8). Although TM6 had a higher average disease score, there was a large reduction after 48 h. Mice treated with ciprofloxacin showed low overall disease scores and looked like the uninfected, untreated mice control after 48 h. After 4 h two untreated mice and one TM6 treated mouse met the euthanasia criteria. After 24 h, four mice from each group were euthanized for CFU enumeration, as was an additional mouse from the TM6 group which met euthanasia criteria. After 48 h, three more untreated mice and one TM1 treated mouse required sacrifice due to high Karnofsky scores. After 72 h, only one untreated mouse and two TM6 treated mice remained, while three TM1 treated, four TM5 treated, and four ciprofloxacin treated mice remained.

Following euthanasia, bacterial load in the lungs and spleen of the mice was evaluated. Untreated mice showed the highest average CFUs/mL in the lungs after 24 h, with 2.2×10^7 CFUs/mL (Fig. 9A). Interestingly, the TM1 treatment group showed the next highest bacterial loads at 1.7×10^7 CFUs/mL, followed by the TM6 treatment group at 1.4×10^7 CFUs/mL. While neither of these trends were statistically significant, mice treated with TM5 showed significantly decreased bacterial CFUs in the lungs, at 4.1×10^6 CFUs/mL, and mice treated with ciprofloxacin showed the greatest decrease in CFUs in the lungs at 6.5×10^4 CFUs/mL. In both ciprofloxacin and TM5 treatment groups, one mouse was determined to be a significant outlier using the Grubb's test for outliers with a p -value of 0.05 and removed from the study. Similarly, one untreated mouse and one ciprofloxacin treated mouse was removed from the spleen dataset as significant outliers. Overall, mice treated with TM6 showed the highest CFUs in the spleen at 1.2×10^6 CFUs/mL, followed by the untreated mice at 1.1×10^6 CFUs/mL and the TM1 treated mice at 1×10^6 CFUs/mL. Peptoid TM5 showed the lowest CFUs/mL for the peptoids tested in the spleen, at 5×10^5 CFUs/mL. Statistical analyses of these data found that none of the groups were significantly different from the untreated mice, despite the presence of a general trend. Ciprofloxacin showed a significant reduction of CFUs/mL in the spleen at 2.9×10^3 CFUs/mL. It should be noted that for both the lungs and spleen, ciprofloxacin-treated mice were able to completely clear infection in two mice after one day for *P. aeruginosa* Xen41.

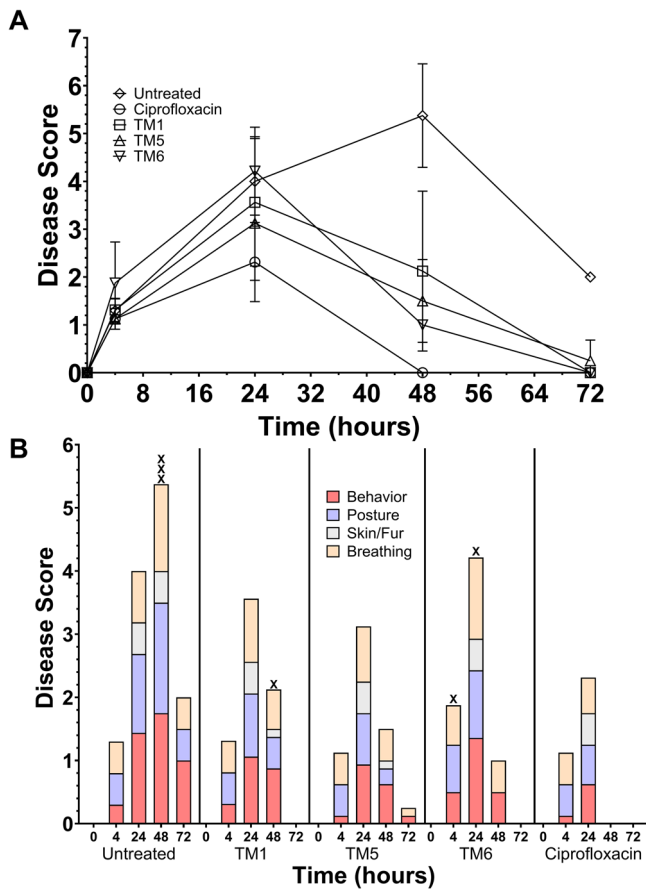


Fig. 8 | Disease scores of mice infected with *P. aeruginosa* Xen41 following peptoid or antibiotic treatment. BALB/c mice were infected with *P. aeruginosa* via the intratracheal route and treated with TM1, TM5, TM6, or ciprofloxacin. A modified Karnofsky score was used to score any adverse effects observed over the course of the infection. **A** Average overall Karnofsky scores for each group of mice tested from 0 h to 72 h, with variance represented as SD. **B** Average Karnofsky scores for each group of mice over time, split into various categories tested. Columns marked with an 'X' indicate where a mouse was sacrificed ahead of schedule.

Throughout all in vivo experiments, mice were monitored via IVIS in vivo imaging to measure bacterial luminescence. Initial experiments showed measurable levels of luminescence in mice 6 h post-infection with 10^7 CFU of Xen41; however, survival rates of these mice were minimal after 24 h (Fig. S4). As a result, a lower dosage of 10^6 CFU was used to infect mice. This dosage was below the IVIS limit of detection, resulting in no measurable signal in vivo. However, necropsy of euthanized animals and subsequent ex vivo imaging of the exposed organs revealed visible differences in all treatment groups compared to the untreated control (Fig. 10).

TM1 and TM5 -treated mice demonstrated increased inflammation and neutrophil recruitment to the site of infection

Histology was performed on all infected mice to determine the effect of both bacterial infection and treatment on the lungs. Several main categories of effect were investigated including purulent inflammation, necrosis, and pulmonary lesion distribution. Blinded histopathological scoring was compared between the individual mice and between the different treatment groups (Fig. 11A, B). Mice treated with ciprofloxacin showed the lowest overall average score of 5.8. TM6 showed the next lowest score, 7.4, followed by untreated mice at 9.6. TM1 showed the second highest score at 13.6 and TM5 had the highest average score at 15.5. Looking at individual mice, all but one of the ciprofloxacin treated mice showed scores under 5 and all but one of the TM6 treated mice

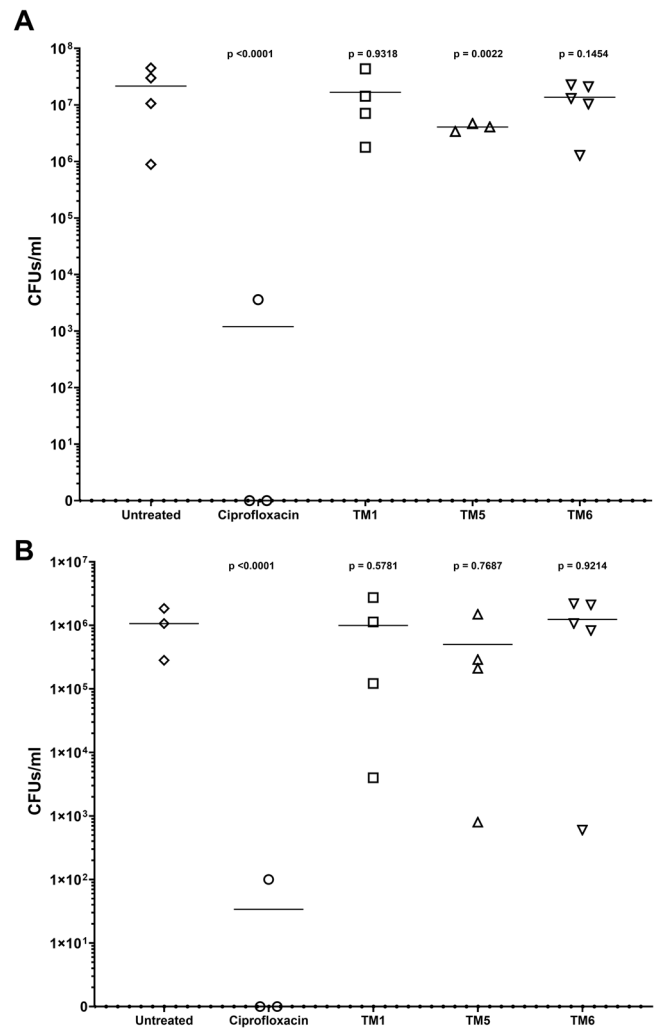


Fig. 9 | Bacterial burdens of *P. aeruginosa* Xen41-infected mice following treatment with peptoid or antibiotic. CFUs taken from sacrifice of day 1 mice. **A** CFUs/ml of Xen41 in the lungs of mice from varying treatment groups. **B** CFUs/ml of Xen41 in the spleen of mice from varying treatment groups. For all graphs, *p*-values are compared to the average of untreated mice. The line across represents the average of all data points within the group.

showed scores under 6. Untreated and TM1 treated mice showed relatively even distribution of scores between mice. TM5 treated mice showed the most consistency across mice, showing identical scores across all mice within the treatment group.

Nearly half of the total histology scoring for TM1 and TM5 mice was purulent bronchiolitis and bronchitis. As a result, computational determination of neutrophils per mm^2 was determined (Fig. 11c)⁵⁶. Despite some variation between mice, ciprofloxacin and TM6 treated mice appeared to have lower levels of neutrophils per mm^2 , between 1800 and 2000, compared to untreated, TM1, or TM5 mice. Untreated, TM1, and TM5 treated mice all had relatively similar counts of neutrophils per mm^2 at about 2500–2800. However, these values were not significantly different. The correlation between increased inflammation and neutrophil recruitment in TM5 treated mice with improved disease scores and bacterial loads leads us to conclude that treatment with peptoids enhanced progression towards the recovery stage of disease. TM6, interestingly, showed the least amount of inflammation in the histology sectioning, while TM1 and TM5 showed high levels of inflammation in various parts of the lung sections (Fig. 12). Ciprofloxacin treated mice also showed low levels of inflammation and untreated mice showed higher inflammation.

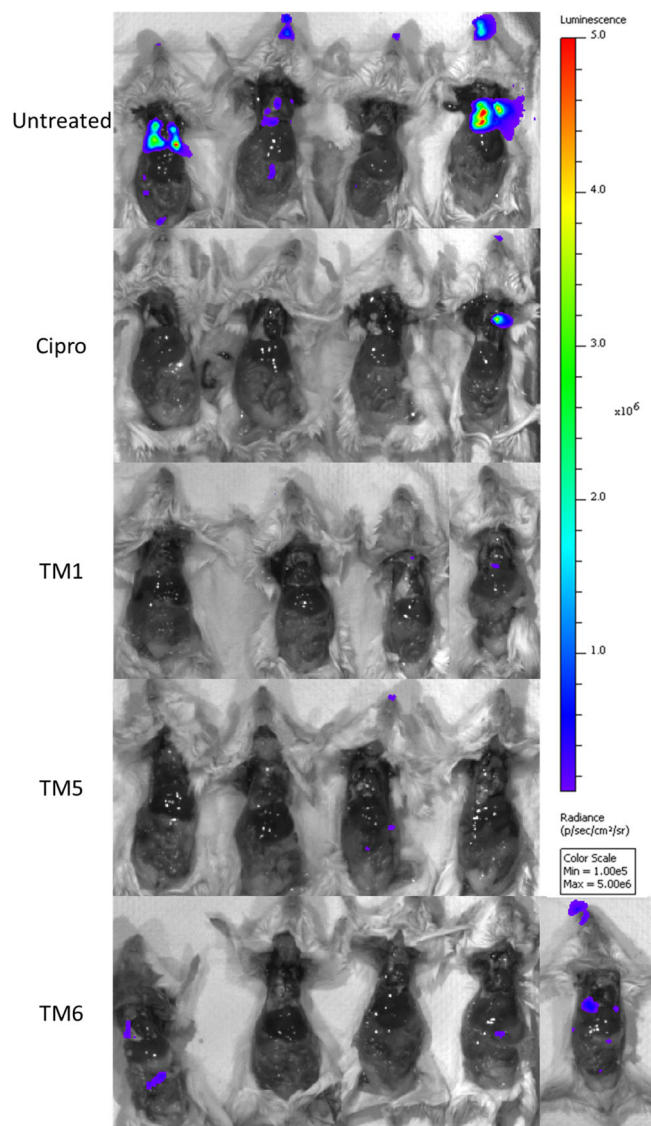


Fig. 10 | IVIS imaging of treated and untreated mice at 24 h post-infection. Images were collected using the same scale of radiance for all mice tested. Each group of mice initially sacrificed were imaged together. An additional mouse in the TM6 group was imaged later using the same scale of radiance as it met the euthanization criteria.

Discussion

The need for novel antimicrobials that are effective against MDR pathogens is well-established as a research imperative. This work addresses this goal by investigating a promising class of potential therapeutics and defining a therapeutic window in which they are effective against *P. aeruginosa* respiratory infections. While a small number of peptide-based antibiotics including polymyxin B, vancomycin, and daptomycin have been approved for clinical use, the development of natural AMPs and their derivatives as antimicrobials has not been easy⁵⁷. Although a number of such drugs have gone through clinical trials, most have not reached clinical use due to their degradation and/or toxicity within a host⁵⁸. The peptoids described here have been specifically designed to prevent degradation by host proteases, and previous work has shown them to be extremely stable^{59,60}. This work also addresses host toxicity, with a focus on a respiratory route of administration, demonstrating that peptoids are a viable treatment option for lung infections. Furthermore, we have demonstrated significant efficacy against *P. aeruginosa* respiratory colonization in an in vivo model, opening the door for development of these peptidomimetics as therapeutics.

To expand upon our previous studies^{37,40,42,61}, we chose to use the bioluminescent strain *P. aeruginosa* Xen41, produced from wild type *P. aeruginosa* PAO1. Bioluminescence requires ATP production, making it an accurate measure of viability, which provides additional unique information beyond that provided by MIC assays performed using standard OD measurements and revealed subtle differences in inhibition with sub-MIC concentrations of TM5 compared to the other peptoids. While all 3 peptoids showed a decrease in luminescence after 4 h of incubation at 1 µg/mL, TM5 shows a 5% larger decrease and a little over 75% reduction of luminescence at 2 µg/mL (Fig. 1A). This suggests that TM5 was more effective at reducing the metabolic activity of *Pseudomonas* at lower concentrations than the other peptoids.

Hydrophobicity and self-assembly have been shown to play important roles in the activity of peptoids. For example, a previous study showed that truncating the 12-mer TM1 to yield the 6-mer TM7 resulted in a near complete loss of activity and self-assembly, while inclusion of a hydrophobic C13 alkyl tail in the 5-mer TM5 results in a very active compound due to increased hydrophobicity³⁶. While the main repeating unit (*N*Lys-*N*spe-*N*spe) is the same in each of these three peptoids, the *N*tridec tail in TM5 may allow improved interaction with bacterial membranes at low concentrations. Furthermore, the alkyl tail facilitates self-assembly into ellipsoidal micelles rather than the helical bundles formed by TM1 or TM6³⁶. As such, it is likely that both hydrophobicity and self-assembly play a larger role in the greater efficacy of TM5 over TM1 and TM6 observed in this study.

In terms of efficacy, TM1 treatment produced a significant reduction in bacterial load at concentrations as low as 0.5 µg/mL, while TM5 showed an overall larger decrease in CFU starting at 2 µg/mL (Fig. 1B). While much of this could be due to experimental variability, the MBC at concentrations of 4 µg/mL remained consistent, supporting the idea that TM5 is more bactericidal at lower concentrations. This finding combined with reduced cytotoxicity led us to select TM5 as our primary candidate against *Pseudomonas*.

To compare peptoid treatment with standard regimens, the traditional antibiotics ciprofloxacin, ceftazidime, meropenem, and kanamycin were also tested in this study. As would be expected of frontline antibiotics, meropenem and ceftazidime were shown to have MIC₉₀s of around 1 µg/mL and MBCs of 2–4 µg/mL (Table 2). Kanamycin, on the other hand, showed an MIC₉₀ of >32 µg/mL and an MBC of >64 µg/mL. The observed differences between MIC and MBC can be explained by the observation that β-lactam antibiotics typically affect peptidoglycan biosynthesis and result in deformation, and subsequent collapse of the bacteria^{62–64}. Ciprofloxacin showed the greatest consistency across MIC and MBC, showing a significant reduction in luminescence, OD and CFUs/mL at concentrations of 0.5 µg/mL and higher (Figs. 2 and 3). As a result, ciprofloxacin was utilized for all in vivo studies as the control antibiotic. Our results are consistent with previously determined MICs/MBCs⁶⁵ and reflect a mechanism of action through inhibition of DNA gyrase⁶⁶.

The time needed for most antibiotics to take effect depends inherently on the mechanism of action and the amount of bacteria present. Our time-to-kill experiments demonstrate that while ciprofloxacin can act within one to two hours of incubation in vitro (Fig. 3B), ceftazidime, meropenem, and kanamycin took more than two hours to produce a measurable decrease in bioluminescence (Fig. S2). In contrast, TM5 treatment produces an immediate reduction of bioluminescence at 5 min for all concentrations at or above the MIC₉₀ (Fig. 3A). After 10 min, TM1 and TM6 show reductions in bioluminescence at their MIC₉₀s (Fig. S1). This is consistent with what was previously observed for *P. aeruginosa* Xen5, suggesting that these peptoids are effective in the same time frame across diverse strains of *P. aeruginosa*⁵⁰. This short timeframe represents a strong advantage over traditional antibiotics.

Another clear advantage over current therapeutics is the lack of resistance emergence observed in our laboratory evolution experiments (Fig. 4). This is consistent with previous studies, which have demonstrated that resistance to antimicrobial peptides is extremely low compared to conventional antibiotics^{37,67}. In addition, we have shown that TM5 is equally

Fig. 11 | Histological analysis of treated and untreated mice. Breakdown of histology scoring as **A** averages of groups with standard error for each category. **C** Neutrophil counts per mm² for histology sections with standard error via computational analysis. Breakdown of histology scoring as **B** individual scoring across several categories for each mouse sacrificed at day 1.

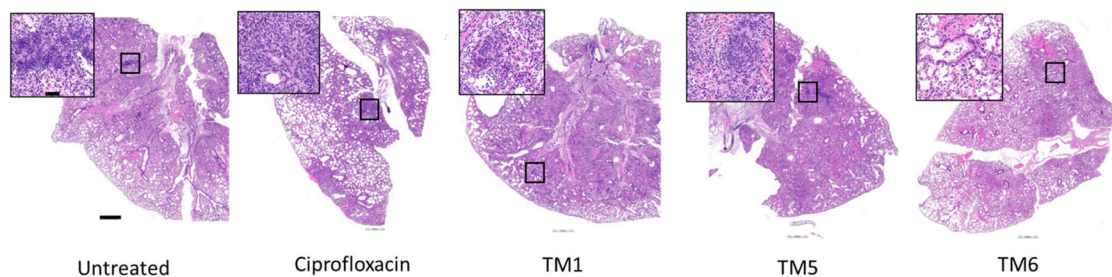
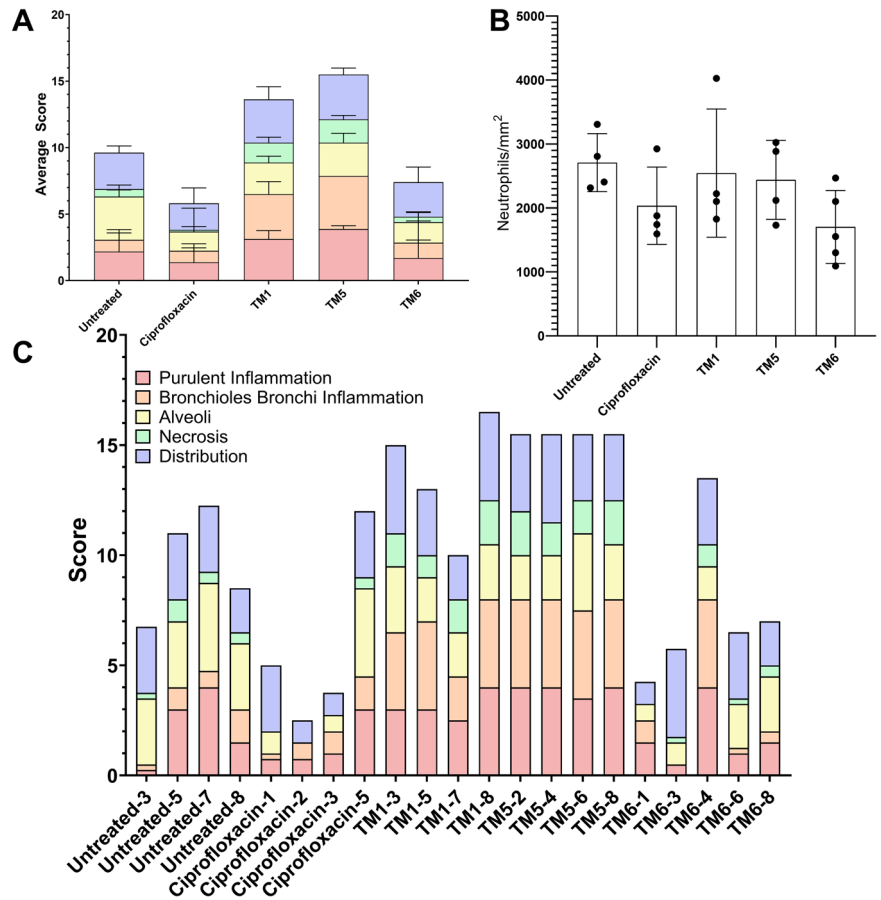


Fig. 12 | Histology sectioning of lungs for representative mice in each treatment group. Histology of H&E-stained tissue sections of lungs for representative mice in each group. Insets are increased magnification of the box seen in the larger image. The short bar, in the inset, is equivalent to 50 μ m and the longer bar is equivalent to 500 μ m.

effective against both antibiotic resistant and susceptible strains, showing no decrease in efficacy against a wide range of clinical strains or evolved strains with full resistance to ciprofloxacin (Fig. 4, Table 3, Fig. S3). As increasing numbers of bacterial infections become resistant to frontline drug treatment, peptoids provide a promising alternative therapy. Moreover, as TM5 has now been demonstrated to be extremely effective against drug resistant strains, it would be interesting to evaluate potential synergy between peptoids and conventional antibiotics for clinical use.

The innate bactericidal properties of our antimicrobial peptoids demonstrated here and in previous studies^{37,40,42,61} suggests that they have promising potential as antimicrobial agents. However, it is important to thoroughly investigate any potential for off-target cytotoxicity against host cells to define a therapeutic window at which the peptoids can safely be used to treat clinical infections. Previous studies have demonstrated high specificity and relatively low cytotoxicity for all three peptoids^{40,61,68}, but cytotoxicity in lung cells had not yet been examined. As *P. aeruginosa* is of

particular concern in lung infections associated with cystic fibrosis, we investigated the effect of TM1, TM5, and TM6 treatment on A549 human lung epithelial cells and demonstrated similar levels of cytotoxicity to L929 mouse fibroblasts and J774 mouse macrophages (Fig. 5, Fig. S4), with peptoids TM5 showing the lowest cytotoxicity with little to no cell death observed at concentrations below 64 μ M.

There has been a growing push towards developing more accurate models of human tissues to evaluate potential therapeutics, including AMPs⁶⁹⁻⁷². In vivo, the epithelial cells that make up the lining of mammalian alveoli grow in a highly polarized fashion within pseudostratified layers that function as a barrier between the airways and interstitial tissue, features that are lost in standard tissue culture. We assayed peptoids cytotoxicity under conditions that more closely model these conditions - spheroids and air-liquid interface (ALI) cultures. Spheroids demonstrate more accurate pharmacokinetics and pharmacodynamics^{73,74}, while ALI cultures allow epithelial cells to differentiate into a similar morphology to that observed

within human alveoli^{75,76}. In both models (Fig. 6), cells show much less cytotoxicity following peptoid treatment than in the cells grown in undifferentiated monolayers. We hypothesize that this is likely due to the formation of tight junctions between cells which decreases the cell surface area exposed to the drug by preventing diffusion of the molecules between cells. For an extracellular pathogen such as *P. aeruginosa*, this would imply that while exposure to the bacteria would remain similar, host cells would have decreased exposure and thus lower side effects. These models suggest that peptoids will be well tolerated by lung epithelial tissues at significantly higher concentrations than previously believed.

To test this hypothesis, we designed an intratracheal drug administration model in BALB/c mice which allowed direct application of peptoids to lung tissues evaluate any negative effects on live animals. For our initial study, we administered doses equivalent to 5X and 10X of the MIC for TM5 and monitored the mice for any ill effects. No significant changes in behaviour or signs of illness were observed at these concentrations, and there was no impact on mouse survival. Therefore, we administered increasing concentrations of TM5 to determine the threshold at which we would begin to observe adverse effects (Fig. 7). We observed no change in behaviour, posture, skin and fur grooming, eye irritation, respiration, gastrointestinal issues, weight, or body temperature above what was observed for the PBS control at 240 μ M concentrations. This is consistent with the parental AMP, LL-37, which has been evaluated in human clinical trials and demonstrated to be safe by oral and topical routes^{77,78}.

As mice were dosed with increasing concentrations, we began to observe transitory effects on respiration and behaviour as would be consistent with minor irritation of the lung tissue above 3.8 mM. This represents concentrations far beyond what would be used in a clinical setting, but nevertheless we observed that all these symptoms had fully resolved within 24–48 h post-inoculation. This suggests that the peptoids are extremely well-tolerated by intratracheal inoculation. In fact, no effects on mortality were observed until the LD₅₀ was reached at a concentration of 10 mM (~20 mg/mL). We have observed that TM5 is soluble in PBS, the buffer used in all peptoid experiments, up to 10 mM. The fact that mortality was observed around the solubility point suggests that any ill effects may have been due to the peptoids precipitating out of solution at this high concentration. Previous work has shown that TM5 self-assembles into well-defined core-shell ellipsoidal micelles with a critical micelle concentration of approximately 1.4 μ M^{37,79}, and it will be of interest in future studies to perform an in depth analysis of how the physicochemical properties of TM5 relate to both efficacy and cytotoxicity. To the best of our knowledge this represents the first demonstration of a well-tolerated peptide-based treatment through intratracheal instillation. The development of novel therapeutics through this route has wide implications for the treatment of lung infections without risk of toxicity to other tissues or through systemic treatment and is likely to be particularly useful in *P. aeruginosa* therapeutics due to the predominance of lung infections with this pathogen in patients with cystic fibrosis.

Since TM5 showed little to no toxicity at 5X MIC levels, the peptoids were tested at this concentration to evaluate in vivo efficacy. Overall, *P. aeruginosa* infected mice treated with TM6, or saline demonstrated poor Karnofsky scores after 24 h, while TM5 and TM1 showed moderate scores at that same time point (Figs. 8 and 9). As would be expected for a frontline antibiotic, ciprofloxacin-treated mice demonstrated the lowest scores, although all mice showed some discomfort after 24 h. All mice showed lower overall Karnofsky scores after 48 h except the untreated mice and all treated mice appeared to show minimal symptoms after 72 h post-treatment, suggesting that at this infectious dose, mice that can survive the initial onset of disease are eventually able to clear the infection.

Live animal imaging was performed throughout the experiment, but the infectious dose of 10⁶ CFU at which at least 50% of the animals are able to survive the infection (LD₅₀) was determined to be below the limit of detection (LOD) for IVIS imaging. *Ex vivo* imaging confirmed bacterial luminescence in the spleens and lungs of uninfected animals, with reduced luminescence in treated animals, but signal could not be quantified

accurately due to nearing the LOD (Fig. 10). In preliminary experiments performed above the 10⁷ CFU LOD, nearly all animals required euthanasia by 24 h, so these experiments were discontinued, despite promising observations with TM5 (Fig S5).

The disease scores observed in all groups correlated well with bacterial burdens. Ciprofloxacin treated mice appeared to have near baseline levels of *P. aeruginosa* in the lungs after 24 h, while TM5 treated mice had significantly reduced CFUs within their lungs (Fig. 9). TM1 and TM6 treated mice did not show a significant reduction in bacterial burden in the lungs, which could explain why they appeared more ill than TM5 and ciprofloxacin-treated mice. Due to the speed at which these peptoids can eliminate bacteria, we hypothesize that some of the higher Karnofsky scoring seen in TM5-treated animals was due to the cytotoxic effects of bacterial killing which would be predicted to lead to an inflammatory response.

This hypothesis is supported by histologic analysis, which showed that TM1 and TM5 treated mice demonstrated high levels of inflammation and increased neutrophil infiltration, while mice treated with ciprofloxacin had lower levels of inflammation and necrosis (Fig. 11). The histology data and reduced CFUs in the lungs in TM5 treated mice suggest that mice were in the later stages of infection, possibly even into the beginning stages of recovery. Alternatively, as the peptoids are derived from LL-37, a natural product of the host immune system that can be conditionally pro-inflammatory and modulate neutrophil recruitment and response to infection, it is possible that TM1 and TM5 produce an immunostimulatory effect that enhances disease recovery^{28,80}. H&E staining of the lung sections suggest that TM6 and ciprofloxacin may have immunosuppressing properties while TM1 and TM5 have immunostimulatory effects (Fig. 12). However, more detailed studies are necessary to discriminate between these potential hypotheses and determine whether peptoids have any impact on neutrophil function.

In this study, we demonstrated the efficacy of TM5, an antimicrobial peptoid, against *P. aeruginosa* Xen41 and several clinical strains, both in vitro and in vivo, with bactericidal activity occurring within a matter of minutes^{40,50}. In addition, our findings demonstrate that the use of air-liquid interface (ALI) cultures or spheroids to test cytotoxicity more accurately represent what is observed in vivo. The use of peptoids similar to TM5 has shown great promise, and as such, may be a valuable source of novel antimicrobials in the fight against antimicrobial resistance. Future studies examining inflammatory markers and immunochemical parameters are warranted to evaluate the use of peptoids as immunomodulators, opening the door to use of potential synergistic interactions between peptoids and conventional antibiotics. These studies would allow for a comprehensive strategy to better understand the mechanisms of peptoids in vivo and ultimately design new, more effective peptoids in the future.

Materials and methods

Peptoid design and synthesis

Peptoid synthesis was performed as previously described in refs. 38,40,81. Briefly, peptoid synthesis was carried out using a Symphony X (Gyros Protein Technologies, Tucson, AZ) peptide synthesizer located at the Molecular Foundry in the Lawrence Berkeley National Laboratory, Berkeley, CA. Peptoids were synthesized on a Rink amide MBHA resin (EMD Biosciences, Gibbstown, NJ). All reagents were purchased from Sigma Aldrich (St. Louis, MO). Synthesis followed the submonomer protocol from Zuckermann, et al.⁸¹. Peptoids were cleaved from the resin by treating with trifluoroacetic acid (TFA):triisopropylsilane:water (95:2.5:2.5 volume ratio) for 10 min. A C18 column in a reversed-phase high performance liquid chromatography (HPLC) system (Waters Corporation, Milford, MA) was used for purification with a linear acetonitrile and water gradient with a compound purity greater than 95% as measured by analytical reverse-phased HPLC. Confirmation of the peptoids synthesis was determined using electrospray ionization mass spectrometry.

Bacterial strains and culture

Bioluminescent Xen 41 *P. aeruginosa*, derived from the parental strain PAO1 (obtained from Xenogen Corp. now part of PerkinElmer, Waltham, MA) was used for all experiments unless otherwise noted. For comparative efficacy experiments, the additional strains PA14, PAZK2019, PAZK69, PAZK3095, PAZK2870 from the Kolter collection (Oxford University), and the clinical isolates PALF05, PA2-22, PA2-67, PA3-9, PA3-17, and PA3-45 described by Kang et al. were used in this study⁴⁹. All strains were streaked onto either cation-adjusted Mueller-Hinton (MH) agar plates or in Luria-Bertani (LB) plates and grown at 37 °C. For each experiment use a single colony was grown overnight in MH or LB broth at 37 °C with shaking at 250 rpm.

MIC and MBC assays

To determine the minimal inhibitory concentration (MIC) of the chosen antibiotics, ceftazidime, ciprofloxacin, kanamycin, and meropenem, and all peptoids, a 96 well plate was setup with triplicates of a 2-fold dilution of the to be tested antimicrobial in MH broth. For antibiotic testing, a polystyrene plate was used while polypropylene plates were used for all peptoids experiments. Overnight cultures of each *P. aeruginosa* strain were diluted 1:100 and grown to log phase (OD₆₀₀ between 0.4–0.9). Log phase cultures were diluted to OD₆₀₀ 0.001 and then added to the plate. The plate containing 2-fold dilution of the antimicrobial and the bacterial strain was incubated overnight at 37 °C. Bacteria and MH broth served as positive controls and just MH broth served as a negative control. The next day, the wells were gently resuspended and luminescence and/or OD₆₀₀ was measured using a plate reader. Unless otherwise noted, MIC is defined by the 95% decrease of the untreated bacteria. Experiments using Xen41 had additional bioluminescence measurements taken at 4 h post-incubation with treatment to measure actively growing bacteria.

To evaluate MBC values, a 10-fold dilution of each sample from the MIC 96 well plate was prepared. The triplicates were plated onto MH agar plates and incubated overnight at 37 °C. The colony forming units (CFUs) were enumerated the next day. All MIC and MBC experiments were performed in triplicate with a minimum of two independent replicates, and representative experiments are shown.

Time-kill assays

To determine how quickly antibiotics and peptoids were able to kill Xen41, a 96 well plate was setup with 3 or 4 replicates of 2-fold dilutions of all tested antimicrobials in MH broth. Log phase cultures were diluted to an OD₆₀₀ of 0.01 before 100 μL of bacteria was added to each well of the plate. Samples were incubated at 37 °C and bioluminescence was measured at the following time points: 0-, 5-, 10-, 15-, 20-, 30-, 45-, 60-, 90-, and 120 min post-addition of bacteria.

Laboratory evolution of resistance

Laboratory evolution of *P. aeruginosa* resistance was performed as has been previously described for antimicrobial peptides⁸². Briefly, 5 mL cultures of *P. aeruginosa* PAO1 were serially passaged in shaking incubators at 37 °C in LB broth containing increasing concentrations of either Ciprofloxacin or peptoids TM5. Strains were sub-cultured daily into fresh media at initial concentrations of antimicrobials starting at 0.5X MIC and doubling weekly until viable bacteria could no longer be recovered from TM5 cultures. Three biological replicates using individual starting cultures were performed for each condition.

Cytotoxicity assays

Cytotoxicity in mammalian cells was measured using an MTS assay as has been previously described⁴⁰. Briefly, A549 human lung epithelial cells, J774.1 mouse macrophage cells, or L927 mouse fibroblasts (ATCC) were cultured in F12K or DMEM media (Gibco) supplemented with 10% FBS. For traditional assays, 10⁴ cells were seeded into each well of a 96-well plate and allowed to adhere for 18 h at which point media was removed and replaced with 2-fold dilutions of peptoids diluted in PBS. Cultures were incubated at 37 °C for 3 h, at which point 20 μL of CellTiter 96 Aqueous Non-Radioactive

cell proliferation assay (Promega) was added to each well. After 2 h of further incubation, the OD490 absorbance was measured using a plate reader. For spheroid cultures, assays were performed as above except that 10⁴ A549 cells were grown in Costar Ultra-Low attachment 96-well plates (Corning) for 72 h at which point spheroids had formed. For ALI cultures, 10⁴ A549 cells were inoculated into Transwell chambers (Corning) and allowed to polarize for 10 days before the apical medial was removed for a further two days before applying the peptoids. All experiments were performed in triplicate, and to confirm the validity of the MTS assay were repeated in independent experiments using an Alamar Blue assay with peptoids diluted in F12K medium containing 10% FBS and incubated overnight for 24 h to evaluate long-term cytotoxicity (Thermo Fisher Scientific).

In vivo toxicity studies

BALB/c mice were treated with increasing dilutions of peptoids suspended in 50 μL PBS via the intratracheal route to evaluate toxicity on the animals using an Endotracheal Intubation Kit (Kent Scientific). Following treatment mice were monitored for survival and scored on a scale of 0–16 for their physical and behavioral responses to peptoids treatment using a modified Karnofsky score at 0, 2, 4, 6, 8, 10, 24, 30, and 48 h post-treatment (Table S1). To control for effects of intubation and liquid administration, control mice were inoculated with either PBS or the parental peptide LL-37 (Anaspec). Two independent experiments were performed with *n* = 2 and *n* = 4 mice per treatment condition respectively.

In vivo efficacy assays

46 BALB/c mice were acclimated for 1 week prior to any experiments in cages of 4, except for two cages of 5 mice. Once acclimated, mice were anesthetized using 2–3% isoflurane with oxygen. All subsequent imaging was carried out using the same anesthetization conditions. Mice were split into treatment groups consisting of 8 total mice per group except for untreated mice which consisted of 10 total mice, and uninfected mice, which consisted of 4 total mice. After anesthetization, mice were given a dosage of 10⁶ bacteria, administered intratracheally using a catheter in 20 μL aliquot. A gentle puff of air was used to ensure bacteria had been disseminated to the lungs before administration of 20 μL of treatment. Untreated mice were given 20 μL of saline to avoid differences in total volume given to the lungs between mice. Mice were then imaged for bioluminescence using an IVIS imaging system. Mice were closely monitored for the next 24 h, with Karnofsky scoring done at 4-, 24-, 48-, and 72 h post-infection. Mice which exceeded 4 points on the modified Karnofsky table were euthanized immediately.

Initially, 1 uninfected and 2 untreated mice were euthanized to get imaging controls as well as baseline numbers of bacteria that had been administered to the lungs. At 24 h, 4 additional mice from each group were randomly selected to be euthanized. The remaining mice were only euthanized if meeting the Karnofsky scoring criteria as mentioned above until 72 h, where all remaining mice were euthanized. For all euthanized mice, imaging was done after opening the mice to expose the lungs and other vital organs using the IVIS system, measuring for bioluminescence. After initial imaging, the lungs, spleen, and liver were harvested and imaged again. Lungs and spleen were then split for histology (stored in 10% neutral buffered formalin), CFUs (stored in PBS), and DNA/RNA isolation (stored in DNA/RNA Shield) and liver was collected for histology (stored in 10% neutral buffered formalin).

Lungs and spleen collected for CFUs were homogenized in PBS and collected for CFU determination. Each sample was serially diluted in 10-fold dilutions (*n* = 3 replicates), plated on LB plates, and incubated at 37 °C overnight. Colonies which formed were counted and CFUs were back calculated.

Histopathology

Following euthanasia, representative samples of lung were collected from each mouse and fixed by immersion in 10% buffered formalin for 48 h at room temperature. Post-fixation, the tissues were stored in 70% ethanol

before embedding in paraffin, sectioned at 5–6 µm, and stained with hematoxylin and eosin to evaluate tissue responses. The whole glass slides of histologic sections were scanned at 20x magnification using the Panoramic Scan II by 3Dhistec (Budapest, Hungary), and analyzed, in a blinded manner, by a board-certified pathologist, and ordinally scored for magnitude of tissue injury, cellular infiltration, inflammation and lesion distribution. Post-acquisition images were uploaded to Aiforia image processing platform (Aiforia Inc., Cambridge, MA) to quantify neutrophils via a validated artificial intelligence/deep learning convolutional neural networks (CNNs) and supervised learning⁵⁶. Statistical analysis of the histopathology ordinal data and neutrophils/mm² was performed by ANOVA using GraphPad Prism.

Statistics and reproducibility

Statistical analysis of the MIC, MBC, and time-kill experiments was performed using 2-way ANOVA, via GraphPad Prism, using Dunnett's multiple comparison test to compare each different concentrations of peptoids or antibiotic used to untreated controls, with standard deviation (SD) shown. For dextran diffusion assays statistical analysis was performed using 2-way ANOVA using Šidák's multiple comparisons test to compare sample means, with standard error mean (SEM) shown. In vivo efficacy experiments were analysed using a 2-way ANOVA test with Tukey's multiple comparisons test to compare CFUs between treatment conditions.

Reporting summary

Further information on research design is available in the Nature Portfolio Reporting Summary linked to this article.

Data availability

The data and results that were generated over the course of this study are included in the published article and the supplementary information. Raw data files have been uploaded to the Figshare repository. The DOI for each figure is listed below. Requests for additional information can be made to the corresponding authors.

Figure 1: <https://doi.org/10.6084/m9.figshare.26384305.v1>

Figure 2: <https://doi.org/10.6084/m9.figshare.26384311.v1>

Figure 3: <https://doi.org/10.6084/m9.figshare.26384314.v1>

Figure 4: <https://doi.org/10.6084/m9.figshare.26384317.v1>

Figure 5: <https://doi.org/10.6084/m9.figshare.26384320.v1>

Figure 6: <https://doi.org/10.6084/m9.figshare.26384338.v1>

Figure 7: <https://doi.org/10.6084/m9.figshare.26384341.v1>

Figure 8: <https://doi.org/10.6084/m9.figshare.26384347.v1>

Figure 9: <https://doi.org/10.6084/m9.figshare.26384353.v1>

Figure 10: <https://doi.org/10.6084/m9.figshare.26384356.v1>

Figure 11: <https://doi.org/10.6084/m9.figshare.26384359.v1>

Figure 12: <https://doi.org/10.6084/m9.figshare.26384365.v1>

Figure S1: <https://doi.org/10.6084/m9.figshare.26384368.v1>

Figure S2: <https://doi.org/10.6084/m9.figshare.26384371.v1>

Figure S3: <https://doi.org/10.6084/m9.figshare.26384374.v1>

Figure S5: <https://doi.org/10.6084/m9.figshare.26384380.v1>

Table 1: <https://doi.org/10.6084/m9.figshare.26384386.v1>

Table 2: <https://doi.org/10.6084/m9.figshare.26384389.v1>

Table 3: <https://doi.org/10.6084/m9.figshare.26384392.v1>

Table S1: <https://doi.org/10.6084/m9.figshare.26384395.v1>

Received: 23 February 2024; Accepted: 13 August 2024;

Published online: 22 August 2024

References

1. WHO, Vol. 2023 (2019).
2. Organization, E.C.f.D.P.a.C.a.W.H. (2023).
3. CDC. (ed. U.S.D.o.H.a.H. Services) (CDC, Atlanta, GA; 2019).
4. Diggle, S. P. & Whiteley, M. Microbe Profile: *Pseudomonas aeruginosa*: opportunistic pathogen and lab rat. *Microbiol. (Read.)* **166**, 30–33 (2020).

5. Belanger, C. R. et al. Identification of novel targets of azithromycin activity against *Pseudomonas aeruginosa* grown in physiologically relevant media. *Proc. Natl Acad. Sci. USA* **117**, 33519–33529 (2020).
6. Hattemer, A. et al. Bacterial and clinical characteristics of health care- and community-acquired bloodstream infections due to *Pseudomonas aeruginosa*. *Antimicrob. Agents Chemother.* **57**, 3969–3975 (2013).
7. Singh, S. B. Confronting the challenges of discovery of novel antibacterial agents. *Bioorg. Med Chem. Lett.* **24**, 3683–3689 (2014).
8. Bassetti, M., Vena, A., Croxatto, A., Righi, E. & Guery, B. How to manage *Pseudomonas aeruginosa* infections. *Drugs Context* **7**, 212527 (2018).
9. Lewis, K. The Science of Antibiotic Discovery. *Cell* **181**, 29–45 (2020).
10. Lewis, K. Platforms for antibiotic discovery. *Nat. Rev. Drug Discov.* **12**, 371–387 (2013).
11. Lewis, K. Antibiotics: Recover the lost art of drug discovery. *Nature* **485**, 439–440 (2012).
12. Alekshun, M. N. & Levy, S. B. Molecular mechanisms of antibacterial multidrug resistance. *Cell* **128**, 1037–1050 (2007).
13. Hancock, R. E. & Sahl, H. G. Antimicrobial and host-defense peptides as new anti-infective therapeutic strategies. *Nat. Biotechnol.* **24**, 1551–1557 (2006).
14. Hancock, R. E. & Lehrer, R. Cationic peptides: a new source of antibiotics. *Trends Biotechnol.* **16**, 82–88 (1998).
15. Jacob, L. & Zasloff, M. Potential therapeutic applications of magainins and other antimicrobial agents of animal origin. *Ciba Found. Symp.* **186**, 197–216 (1994). discussion 216–123.
16. Chertov, O. et al. Identification of defensin-1, defensin-2, and CAP37/azurocidin as T-cell chemoattractant proteins released from interleukin-8-stimulated neutrophils. *J. Biol. Chem.* **271**, 2935–2940 (1996).
17. Mookherjee, N. et al. Modulation of the TLR-mediated inflammatory response by the endogenous human host defense peptide LL-37. *J. Immunol.* **176**, 2455–2464 (2006).
18. Niyonsaba, F., Ushio, H., Nagaoka, I., Okumura, K. & Ogawa, H. The human beta-defensins (–1, –2, –3, –4) and cathelicidin LL-37 induce IL-18 secretion through p38 and ERK MAPK activation in primary human keratinocytes. *J. Immunol.* **175**, 1776–1784 (2005).
19. Scott, M. G., Davidson, D. J., Gold, M. R., Bowdish, D. & Hancock, R. E. W. The human antimicrobial peptide LL-37 is a multifunctional modulator of innate immune responses. *J. Immunol.* **169**, 3883–3891 (2002).
20. Oppenheim, F. G. et al. Histatins, a novel family of histidine-rich proteins in human parotid secretion. Isolation, characterization, primary structure, and fungistatic effects on *Candida albicans*. *J. Biol. Chem.* **263**, 7472–7477 (1988).
21. Kosciuzuk, E. M. et al. Cathelicidins: family of antimicrobial peptides. A review. *Mol. Biol. Rep.* **39**, 10957–10970 (2012).
22. Ganz, T., Selsted, M. E. & Lehrer, R. I. Defensins. *Eur. J. Haematol.* **44**, 1–8 (1990).
23. Lai, Y. & Gallo, R. L. AMPed up immunity: how antimicrobial peptides have multiple roles in immune defense. *Trends Immunol.* **30**, 131–141 (2009).
24. Howell, M. et al. Exploring synergy and its role in antimicrobial peptide biology. *Methods Enzymol.* **663**, 99–130 (2022).
25. Durr, U. H., Sudheendra, U. S. & Ramamoorthy, A. LL-37, the only human member of the cathelicidin family of antimicrobial peptides. *Biochim Biophys. Acta* **1758**, 1408–1425 (2006).
26. Patch, J. A. & Barron, A. E. Mimicry of bioactive peptides via non-natural, sequence-specific peptidomimetic oligomers. *Curr. Opin. Chem. Biol.* **6**, 872–877 (2002).
27. Nijnik, A. & Hancock, R. Host defence peptides: antimicrobial and immunomodulatory activity and potential applications for tackling antibiotic-resistant infections. *Emerg. Health Threats J.* **2**, e1 (2009).

28. Kahlenberg, J. M. & Kaplan, M. J. Little peptide, big effects: the role of LL-37 in inflammation and autoimmune disease. *J. Immunol.* **191**, 4895–4901 (2013).
29. Santos, J., Ventura, S. & Pallares, I. LL-37 and CsgC exemplify the crosstalk between anti-amyloid, antimicrobial, and anti-biofilm protein activities. *Neural Regen. Res* **18**, 1027–1028 (2023).
30. Yang, X. et al. LL-37-Induced Autophagy Contributed to the Elimination of Live *Porphyromonas gingivalis* Internalized in Keratinocytes. *Front Cell Infect. Microbiol* **10**, 561761 (2020).
31. Biswas, D. et al. LL-37-mediated activation of host receptors is critical for defense against group A streptococcal infection. *Cell Rep.* **34**, 108766 (2021).
32. Fabisiak, A., Murawska, N. & Fichna, J. LL-37: Cathelicidin-related antimicrobial peptide with pleiotropic activity. *Pharm. Rep.* **68**, 802–808 (2016).
33. Neshani, A. et al. LL-37: Review of antimicrobial profile against sensitive and antibiotic-resistant human bacterial pathogens. *Gene Reports* **17** (2019).
34. Rodriguez-Rojas, A., Baeder, D. Y., Johnston, P., Regoes, R. R. & Rolff, J. Bacteria primed by antimicrobial peptides develop tolerance and persist. *PLoS Pathog.* **17**, e1009443 (2021).
35. He, J., Starr, C. G. & Wimley, W. C. A lack of synergy between membrane-permeabilizing cationic antimicrobial peptides and conventional antibiotics. *Biochim Biophys. Acta* **1848**, 8–15 (2015).
36. Josefine et al. Self-assembly of antimicrobial peptoids impacts their biological effects on ESKAPE bacterial pathogens. *ACS Infect Dis* (2022).
37. Lin, J. S. et al. Anti-persister and Anti-biofilm Activity of Self-Assembled Antimicrobial Peptoid Ellipsoidal Micelles. *ACS Infect. Dis.* **8**, 1823–1830 (2022).
38. Diamond, G. et al. Potent Antiviral Activity against HSV-1 and SARS-CoV-2 by Antimicrobial Peptides. *Pharm. (Basel)* **14**, 304 (2021).
39. Kumar, V. et al. Membrane-acting biomimetic peptoids against visceral leishmaniasis. *FEBS Open Bio* **13**, 519–531 (2023).
40. Benjamin, A. B. et al. Efficacy of Cathelicidin-Mimetic Antimicrobial Peptoids against *Staphylococcus aureus*. *Microbiol Spectr.* **10**, e0053422 (2022).
41. Chongsiriwatana, N. P. & Barron, A. E. Comparing Bacterial Membrane Interactions of Antimicrobial Peptides and Their Mimics. *Antimicrobial. Peptides: Methods Protoc.* **618**, 171–182 (2010).
42. Kapoor, R. et al. Antimicrobial peptoids are effective against *Pseudomonas aeruginosa* biofilms. *Antimicrob. Agents Chemother.* **55**, 3054–3057 (2011).
43. Fink, A., Schwab, D. & Papousek, I. Sensitivity of EEG upper alpha activity to cognitive and affective creativity interventions. *Int J. Psychophysiol.* **82**, 233–239 (2011).
44. Thompson, J. M. et al. Mouse model of Gram-negative prosthetic joint infection reveals therapeutic targets. *JCI Insight* **3**, e121737 (2018).
45. Grace, A., Sahu, R., Owen, D. R. & Dennis, V. A. *Pseudomonas aeruginosa* reference strains PAO1 and PA14: A genomic, phenotypic, and therapeutic review. *Front Microbiol* **13**, 1023523 (2022).
46. Chandler, C. E. et al. Genomic and Phenotypic Diversity among Ten Laboratory Isolates of *J Bacteriol* **201** (2019).
47. O'Toole, G. A. & Kolter, R. Flagellar and twitching motility are necessary for *Pseudomonas aeruginosa* biofilm development. *Mol. Microbiol* **30**, 295–304 (1998).
48. Oliveira, N. M. et al. Biofilm Formation As a Response to Ecological Competition. *PLoS Biol.* **13**, e1002191 (2015).
49. Kang, D. et al. Pyoverdine-Dependent Virulence of *Pseudomonas aeruginosa* Isolates From Cystic Fibrosis Patients. *Front Microbiol* **10**, 2048 (2019).
50. Chongsiriwatana, N. P. et al. Intracellular biomass flocculation as a key mechanism of rapid bacterial killing by cationic, amphipathic antimicrobial peptides and peptoids. *Sci. Rep.* **7**, 16718 (2017).
51. Kadurugamuwa, J. L. et al. Direct continuous method for monitoring biofilm infection in a mouse model. *Infect. Immun.* **71**, 882–890 (2003).
52. Cadavid-Vargas, J. F. et al. 6-Methoxyquinoline complexes as lung carcinoma agents: induction of oxidative damage on A549 monolayer and multicellular spheroid model. *J. Biol. Inorg. Chem.* **24**, 271–285 (2019).
53. Wang, Y. et al. DNA Origami Penetration in Cell Spheroid Tissue Models is Enhanced by Wireframe Design. *Adv. Mater.* **33**, e2008457 (2021).
54. Fukuda, Y. et al. Layer-by-layer cell coating technique using extracellular matrix facilitates rapid fabrication and function of pancreatic beta-cell spheroids. *Biomaterials* **160**, 82–91 (2018).
55. Saleh, F., Harb, A., Soudani, N. & Zaraket, H. A three-dimensional A549 cell culture model to study respiratory syncytial virus infections. *J. Infect. Public Health* **13**, 1142–1147 (2020).
56. Bencosme-Cuevas, E. et al. Ixodes scapularis nymph saliva protein blocks host inflammation and complement-mediated killing of Lyme disease agent, *Borrelia burgdorferi*. *Front Cell Infect. Microbiol* **13**, 1253670 (2023).
57. Rončević, T., Puizina, J. & Tossi, A. Antimicrobial Peptides as Anti-Infective Agents in Pre-Post-Antibiotic Era? *Int J. Mol. Sci.* **20**, 5713 (2019).
58. Dijksteel, G. S., Ulrich, M. M. W., Middelkoop, E. & Boekema, B. K. H. L. Review: Lessons Learned From Clinical Trials Using Antimicrobial Peptides (AMPs). *Front Microbiol* **12**, 616979 (2021).
59. Sanborn, T. J., Wu, C. W., Zuckermann, R. N. & Barron, A. E. Extreme stability of helices formed by water-soluble poly-N-substituted glycines (polypeptoids) with alpha-chiral side chains. *Biopolymers* **63**, 12–20 (2002).
60. Czyzewski, A. M. et al. In vivo, in vitro, and in silico characterization of peptoids as antimicrobial agents. *PLoS One* **11**, e0135961 (2016).
61. Chongsiriwatana, N. P. et al. Peptoids that mimic the structure, function, and mechanism of helical antimicrobial peptides. *Proc. Natl. Acad. Sci. USA* **105**, 2794–2799 (2008).
62. Mosley, J. F. 2nd et al. Ceftazidime-avibactam (Avycaz): for the treatment of complicated intra-abdominal and urinary tract infections. *P T* **41**, 479–483 (2016).
63. Hayes, M. V. & Orr, D. C. Mode of action of ceftazidime: affinity for the penicillin-binding proteins of *Escherichia coli* K12, *Pseudomonas aeruginosa* and *Staphylococcus aureus*. *J. Antimicrob. Chemother.* **12**, 119–126 (1983).
64. Dhillon, S. Meropenem/Vaborbactam: a review in complicated urinary tract infections. *Drugs* **78**, 1259–1270 (2018).
65. Day, C. A., Marceau-Day, M. L. & Day, D. F. Increased susceptibility of *Pseudomonas aeruginosa* to ciprofloxacin in the presence of vancomycin. *Antimicrob. Agents Chemother.* **37**, 2506–2508 (1993).
66. LeBel, M. Ciprofloxacin: chemistry, mechanism of action, resistance, antimicrobial spectrum, pharmacokinetics, clinical trials, and adverse reactions. *Pharmacotherapy* **8**, 3–33 (1988).
67. Spohn, R. et al. Integrated evolutionary analysis reveals antimicrobial peptides with limited resistance. *Nat. Commun.* **10**, 4538 (2019).
68. Lee, J. et al. Effect of side chain hydrophobicity and cationic charge on antimicrobial activity and cytotoxicity of helical peptoids. *Bioorg. Med Chem. Lett.* **28**, 170–173 (2018).
69. Vandana, J. J., Manrique, C., Lacko, L. A. & Chen, S. Human pluripotent-stem-cell-derived organoids for drug discovery and evaluation. *Cell Stem Cell* **30**, 571–591 (2023).
70. Choi, K. G., Wu, B. C., Lee, A. H., Baquir, B. & Hancock, R. E. W. Utilizing Organoid and Air-Liquid Interface Models as a Screening Method in the Development of New Host Defense Peptides. *Front Cell Infect. Microbiol* **10**, 228 (2020).
71. Langhans, S. A. Three-Dimensional. *Front Pharm.* **9**, 6 (2018).
72. Sperle, K., Pochan, D. J. & Langhans, S. A. 3D Hydrogel Cultures for High-Throughput Drug Discovery. *Methods Mol. Biol.* **2614**, 369–381 (2023).

73. Mizoi, K. et al. Utility of Three-Dimensional Cultures of Primary Human Hepatocytes (Spheroids) as Pharmacokinetic Models. *Biomedicines* **8**, 374 (2020).
74. Proctor, W. R. et al. Utility of spherical human liver microtissues for prediction of clinical drug-induced liver injury. *Arch. Toxicol.* **91**, 2849–2863 (2017).
75. Baldassi, D., Gabold, B. & Merkel, O. Air-liquid interface cultures of the healthy and diseased human respiratory tract: promises, challenges and future directions. *Adv. Nanobiomed Res.* **1**, 2000111 (2021).
76. Lee, R. E. et al. Air-Liquid interface cultures to model drug delivery through the mucociliary epithelial barrier. *Adv. Drug Deliv. Rev.* **198**, 114866 (2023).
77. Zhang, H. et al. Preliminary evaluation of the safety and efficacy of oral human antimicrobial peptide LL-37 in the treatment of patients of COVID-19, a small-scale, single-arm, exploratory safety study. *medRxiv*, <https://doi.org/10.1101/2020.05.11.20064584> (2020).
78. Grönberg, A., Mahlapuu, M., Stähle, M., Whately-Smith, C. & Rollman, O. Treatment with LL-37 is safe and effective in enhancing healing of hard-to-heal venous leg ulcers: a randomized, placebo-controlled clinical trial. *Wound Repair Regen.* **22**, 613–621 (2014).
79. Chongsiriwatana, N. P. et al. Short alkylated peptoid mimics of antimicrobial lipopeptides. *Antimicrob. Agents Chemother.* **55**, 417–420 (2011).
80. Alalwani, S. M. et al. The antimicrobial peptide LL-37 modulates the inflammatory and host defense response of human neutrophils. *Eur. J. Immunol.* **40**, 1118–1126 (2010).
81. Zuckermann, R. N., Kerr, J. M., Kent, S. B. H. & Moos, W. H. Efficient method for the preparation of peptoids [Oligo(N-Substituted Glycines)] by submonomer solid-phase synthesis. *J. Am. Chem. Soc.* **114**, 10646–10647 (1992).
82. Jochumsen, N. et al. The evolution of antimicrobial peptide resistance in *Pseudomonas aeruginosa* is shaped by strong epistatic interactions. *Nat. Commun.* **7**, 13002 (2016).
- data development and paper editing. A.E.B. and J.D.C. were involved in paper editing, project formulation and management, and project funding.

Competing interests

A.E.B. is a shareholder and former member of the Board of Directors of Maxwell Biosciences, Inc., which is developing the antimicrobial peptoids for clinical use. JDC is also a shareholder in Maxwell Biosciences Inc. No employee of Maxwell Biosciences had any role in the design of the study; in the collection, analyses, or interpretation of data; in the writing of the manuscript, or in the decision to publish the results.

Ethics

All protocols were approved (IACUC 2021-0201 M) by the Texas A&M University Institutional Animal Care and Use Committee. All authors of this study have fulfilled the criteria for authorship required by Nature Portfolio journals and participated in the design and implementation of the study.

Additional information

Supplementary information The online version contains supplementary material available at <https://doi.org/10.1038/s42003-024-06725-1>.

Correspondence and requests for materials should be addressed to Annelise E. Barron or Jeffrey D. Cirillo.

Peer review information *Communications Biology* thanks the anonymous reviewers for their contribution to the peer review of this work. Primary Handling Editor: Tobias Goris.

Reprints and permissions information is available at <http://www.nature.com/reprints>

Publisher's note Springer Nature remains neutral with regard to jurisdictional claims in published maps and institutional affiliations.

Open Access This article is licensed under a Creative Commons Attribution-NonCommercial-NoDerivatives 4.0 International License, which permits any non-commercial use, sharing, distribution and reproduction in any medium or format, as long as you give appropriate credit to the original author(s) and the source, provide a link to the Creative Commons licence, and indicate if you modified the licensed material. You do not have permission under this licence to share adapted material derived from this article or parts of it. The images or other third party material in this article are included in the article's Creative Commons licence, unless indicated otherwise in a credit line to the material. If material is not included in the article's Creative Commons licence and your intended use is not permitted by statutory regulation or exceeds the permitted use, you will need to obtain permission directly from the copyright holder. To view a copy of this licence, visit <http://creativecommons.org/licenses/by-nc-nd/4.0/>.

© The Author(s) 2024

Acknowledgements

A.E.B. thanks the NIH for funding this work with a Director's Pioneer Award, grant # 1DP1 OD029517. A.E.B. also acknowledges funding from Stanford University's Discovery Innovation Fund, the Cisco University Research Program Fund, and the Silicon Valley Community Foundation, and Dr. James J. Truchard and the Truchard Foundation. J.D.C. thanks the NIH for providing additional funding for this project through grants number AI149383 and EB032983. M.G.M. and M.L.B. thank the Medical Research Council for providing additional funding through the MRC Precision Medicine Doctoral Training Programme. We gratefully acknowledge Dr. Michael Connolly and Dr. Behzad Rad at the Molecular Foundry for assistance with peptoids synthesis and sample preparation equipment. Work at the Molecular Foundry was supported by the Office of Science, Office of Basic Energy Sciences, of the U.S. Department of Energy under Contract No. DE-AC02-05CH11231.

Author contributions

Within this work, M.G.M and A.B.B. both contributed in data development, analysis, paper writing and editing, and project formulation. M.L.B., C.H., M.L., J.S.L, K.J.K., N.W., L.G.A., S.B., R.M.M., and C.L.C. were all involved in